Spectrum Sensing for Wireless Microphone Signals using Multiple Antennas

Daniel Romero, *Student Member, IEEE,* and Roberto López-Valcarce, *Member, IEEE,*

***Abstract*—Spectrum sensors for cognitive radio are expected to deploy multiple antennas in order to overcome the noise uncertainty problem and minimize the effects of small-scale fading. Despite the requirement that these sensors must detect wireless microphone (WM) signals, works in the literature have focused either on general purpose multiantenna detectors, or single antenna WM detectors. We exploit the spatial structure and particular properties of WM waveforms to derive four multiantenna detectors for WM signals with different performance/complexity tradeoffs. These detectors are based on the generalized likelihood ratio test, which is derived under several signal models exploiting either the fact that the bandwidth of a WM signal never exceeds 200 kHz, the property that these signals have a constant magnitude, or both.**

The proposed detectors do not require synchronization with the WM signal and are robust to the noise uncertainty problem as well as to small-scale fading. Using the simulation guidelines from the IEEE 802.22 standard, the novel multiantenna WM detectors are shown to outperform previous schemes, thus demonstrating the advantages of exploiting spatial correlation along with WM signal structure.

***Index Terms*—Communication, communication channels, signal detection, signal processing.**

I. Introduction

RECENT regulations in the United States allow unlicensed wireless devices to operate in the broadcast television spectrum at locations where that spectrum is unused by authorized services [1]–[3]. These services include, among others, television broadcast stations and low-power auxiliary devices such as wireless microphones (WMs). While the current state of these regulations establishes that unlicensed users must determine the occupancy of the radio spectrum by means of a geo-location database, the Federal Communications Commission (FCC) encourages the development of spectrum sensing procedures to detect the presence of the incumbent services, which is expected to improve spectrum efficiency in the future [2]. Furthermore, the IEEE standard 802.22 [4] explicitly demands sensing mechanisms for detecting WM signals.

The authors are with the Department of Signal Theory and Communications, University of Vigo, 36310 Vigo, Spain (email: dromero@gts.uvigo.es, valcarce@gts.uvigo.es).

This work has been jointly supported by the Galician Government, the Spanish Government and the European Regional Development Fund (ERDF) under the FPU grant AP2010-0149, the TACTICA project, the DYNACS project (TEC2010- 21245-C02/TCM), the COMONSENS project (CONSOLIDER-INGENIO 2010 CSD2008-00010), and the agreement for funding the Atlantic Research Center for Information and Communication Technologies (AtlantTIC).

Part of this work has been presented at the 2011 IEEE 12th Int. Workshop on Signal Processing Advances in Wireless Communications.

The spectrum access scheme described above is commonly referred to as dynamic spectrum access [5] or, more frequently, cognitive radio [6], [7], and constitutes an emerging technology for vehicular devices (see [8]–[10] and references therein). In this context we usually refer to the incumbent transmitters as *primary users*, whereas the opportunistic devices are known as the *secondary users*, which must sense the channel prior to transmitting and decide, in view of the observations, whether the primary users are present or not. Decision rules are termed *detectors* and can be based on one or more features of the primary signal and the noise.

One such feature is energy: if we know the noise power, we can just measure the strength of the received signal and declare the channel as busy if the measurement is high relative to the noise power. This simple procedure is termed energy detection [11] and is optimal in settings without further knowledge of the signal structure. However, this detector is unable to detect signals in the low signal-to-noise ratio (SNR) regime since an accurate knowledge of the noise power is seldom available in practice [9], [12], [13]. In fact, the practical interest of this scheme may be limited since the FCC establishes that any secondary device operating in the TV band must be able to detect signals at -114 dBm, which means that the SNR may be as low as -20 dB [12], [14]. This fact has motivated detectors exploiting other properties of the primary signal such as spectral flatness, amplitude properties, spatial correlation, etc. (see [6], [7] and the references therein). Detectors not requiring noise power knowledge are characterized by the fact that they are invariant to scalings [15], [16] and are termed *constant false alarm rate* (CFAR) detectors, since their probability of false alarm does not depend on the noise power [11]. For the reasons above, using CFAR detectors is highly convenient from a practical point of view.

In the context of detection of WM signals, both CFAR and non-CFAR schemes have been proposed in the literature. Among the CFAR detectors we mention the detector by Xu *et al.* [17], which makes a decision based on the ratios of consecutive singular values of a Hankel matrix containing the received samples; and the detector by Hassan and Nasr [18], where the decisions of two statistics are combined, one of which is CFAR whereas the other is not, and the threshold is adapted accordingly. Among the non-CFAR detectors we mention that in [19], where the test statistic is the output of a matched filter in the autocorrelation domain; the detectors in [20] and [21], which are, respectively, the maximum of the standard periodogram and Welch periodogram; and the detector in [22], which uses the Teager-Kaiser energy operator to exploit the constant magnitude property of the signal.

All the detectors above are single-antenna schemes. However, cognitive radios are expected to deploy multiple antennas because of their advantages for both communication (since they provide multiplexing and diversity gains) and spectrum sensing [12], [23], enabling detectors which are fast, resilient to small-scale fading and robust to the noise uncertainty problem discussed above (i.e., CFAR detectors). A number of multiantenna detectors have been proposed in the past. Some of them exploit exclusively the spatial structure of the signal, such as the detector in [24], which only exploits spatial independence of the noise, and the detector in [10], [23], [25], which in addition assumes that the signal subspace has dimension one. Generalizations to signal subspaces of larger dimension were proposed in [26]. Other schemes exploit both spatial and temporal structure by assuming that the signal has a power spectral density (PSD) that is known up to a scaling [27], [28]. We also mention the *ad-hoc* detectors in [14], which exploit the fact that the noise process is temporally and spatially uncorrelated.

Whereas the above multiantenna schemes could be readily applied for WM signal detection, none of them fully exploits the prior information that is available regarding WM signal structure. To the best of our knowledge, no multiantenna detectors have been proposed specifically targeting WM signals. We fill this gap by proposing multiantenna detectors for WMs which exploit the available *a priori* knowledge about the structure of these signals.

In particular, note that in the framework of the IEEE 802.22 standard, a 6 MHz TV channel is scanned for the presence of TV and WM signals, among others. This motivates acquiring a 6 MHz-wide channel and applying different detection algorithms for each kind of signals that may be present. Since WM transmissions are confined to a bandwidth of 200 kHz [22], [29], [30], it is reasonable to take advantage of the fact that the signal to be detected has a small bandwidth relative to the 6 MHz operational bandwidth. In other words, we may exploit the fact that the signal is *bandlimited* (BL). Moreover, regulations dictate that the carrier frequency of WM transmissions must be a multiple of 25 kHz away from the channel edge [31], meaning that the possible frequency locations of WM signals are known *a priori*. Additionally, WM wavefoms typically employ the analog frequency modulation (FM) [19], [29], and therefore their complex lowpass equivalent exhibits a constant magnitude (CM).

We consider these two features, namely the BL and CM properties, along with spatial information in order to develop several multiantenna detectors for WMs. These detectors differ in the amount of prior information they exploit, which provides the user with different tradeoffs between performance and complexity. In order to cope with unknown parameters, our derivations apply the Generalized Likelihood Ratio (GLR) framework [11], [15] to different signal models. The deterministic approach followed, where the signal term is modeled as a deterministic unknown parameter [11], [15], [25], results in robust and general detectors since no assumptions are made about the statistical distribution of the transmitted signal or the channel. Moreover, this approach allows gradually incorporating prior information about WMs while keeping the problem mathematically tractable. To sum up, this paper is, to the best of our knowledge, the first one to provide multiantenna detection rules specifically tailored to detect WM signals. These rules are robust and general since they do not require signal or channel statistical information, and trade performance for complexity.

The detectors derived in this paper generalize those in [10], [23], [25], [32]–[34] and were especially inspired by the work in [32], [33]. Moreover, these detectors can also be used in other settings where BL or CM signals need to be detected. Examples of CM signals include those modulated with Frequency Shift Keying (FSK), Continuous Phase Modulation (CPM), Gaussian Minimum Shift Keying (GMSK), which is employed in the GSM cellular system, etc.

The paper is organized as follows. The problem is formulated in Sec. II, where the deterministic signal model is presented along with an introduction to the GLR test. We then derive several detectors that exploit different degrees of prior information:

- In Sec. III we derive the GLR test for the case where only the BL property is exploited, resulting in the simplest of all detectors proposed in the paper. Next, we consider both the BL property and the spatial rank-1 structure of the WM signal to derive another GLR detector[1].
- In Sec. IV, the CM property is exploited along with the rank-1 space structure of the WM signal to derive a third detector.
- The multiantenna GLR test that jointly exploits the BL and CM properties, along with the spatial structure, is developed in Sec. V. This detector provides the best performance since it exploits all prior information, although this is at the expense of the highest computational complexity.

Some common considerations and implementation issues are discussed in Sec. VI, and performance is analytically evaluated in Sec. VII. In Sec. VIII we assess performance using the simulation guidelines for WMs provided by the IEEE 802.22 working group. Concluding remarks are given in Sec. IX.

Notation: Vectors and matrices are denoted by boldface lowercase and uppercase letters, respectively. Superscripts *, ^{T} and ^{H} respectively denote conjugate, transpose, and conjugate transpose. The tilde $\tilde{}$ is used to denote frequency-domain variables. The trace and expectation are represented by $\mathrm{Tr}\,(\cdot)$ and $\mathrm{E}\,\{\cdot\}$, respectively. The symbol "$\star$" is used to denote convolution whereas $\delta[n]$ represents the Kronecker delta function. The ℓ^p-norm of a vector is denoted by $||\cdot||_p$; the subscript will be usually omitted for the Euclidean (ℓ^2) norm. For a matrix $\boldsymbol{A} \in \mathbb{C}^{m\times n}$, the Frobenius norm is defined as $||\boldsymbol{A}||_F = \sqrt{\mathrm{Tr}\,(\boldsymbol{A}\boldsymbol{A}^H)}$, whereas the *operator norm*[2] induced by $||\cdot||_p$ on $\mathbb{C}^n$ and $||\cdot||_q$ on $\mathbb{C}^m$ is denoted by $||\boldsymbol{A}||_{p,q}$, i.e., $||\boldsymbol{A}||_{p,q} = \max_{\boldsymbol{x}} ||\boldsymbol{A}\boldsymbol{x}||_q$ subject to $||\boldsymbol{x}||_p = 1$.

[1] As usual, the terms *detector* and *test* will be used interchangeably throughout the paper.

[2] Also known in some contexts as dual norm or subordinate norm.

II. Problem setting

A. Signal model

Consider a sensor with M antennas that selects, downconverts and samples some frequency channel at f_s samples/s. If a WM signal $x^*[n]$ is present[3], then the n-th sample at the m-th antenna is given by

$$y_m[n] = x^*[n] \star h_m[n] + w_m[n], \quad m = 0, 1, \ldots, M-1, \quad n = 0, 1, \ldots, N-1,$$

where N is the number of samples per antenna, $h_m[n]$ is the impulse response of the channel from the primary transmitter to the m-th antenna, and $w_m[n]$ is the noise, which is assumed zero-mean, circularly symmetric Gaussian, and temporally and spatially white, i.e., $\mathrm{E}\left\{w_m[n]w_p^*[q]\right\} = \sigma^2\delta[m-p]\delta[n-q]$. Let $\boldsymbol{h}[n] \doteq [\ h_0[n] \ \ \ldots \ \ h_{M-1}[n]\ ]^T$ and $\boldsymbol{q}[n] \doteq x^*[n] \star \boldsymbol{h}[n] = \sum_k x^*[n-k]\boldsymbol{h}[k]$. Introducing the $M \times N$ matrix $\boldsymbol{Q} \doteq [\ \boldsymbol{q}[0] \ \ \ldots \ \ \boldsymbol{q}[N-1]\ ]$, we can write $\boldsymbol{Y} = \boldsymbol{Q} + \boldsymbol{W}$, where the (m, n) entries of $\boldsymbol{Y}$ and $\boldsymbol{W}$ are respectively $y_m[n]$ and $w_m[n]$.

The problem is to decide on the presence or absence of the signal $x^*[n]$, thus testing the null hypothesis $\mathcal{H}_0$ that the received signal is noise only, i.e. $\boldsymbol{Y} = \boldsymbol{W}$, against the alternative $\mathcal{H}_1$ stating that there is both signal and noise, i.e. $\boldsymbol{Y} = \boldsymbol{Q} + \boldsymbol{W}$. The transmitted signal $x^*[n]$, the channel coefficients $h_m[n]$ and the noise power σ^2 are modeled as deterministic unknown parameters [11], which will allow us to gradually introduce the prior information available about $x^*[n]$ and $h_m[n]$. According to this assumption, the observations in $\boldsymbol{Y}$ are Gaussian distributed, with $\mathrm{E}\{\boldsymbol{Y} \mid \mathcal{H}_0\} = \boldsymbol{0}$ and $\mathrm{E}\{\boldsymbol{Y} \mid \mathcal{H}_1\} = \boldsymbol{Q}$. Let

$$\hat{\boldsymbol{R}}_0 \doteq \frac{1}{N}\boldsymbol{Y}\boldsymbol{Y}^H, \quad \hat{\boldsymbol{R}}_1 \doteq \frac{1}{N}(\boldsymbol{Y}-\boldsymbol{Q})(\boldsymbol{Y}-\boldsymbol{Q})^H \tag{1}$$

respectively denote the sample spatial covariance matrices under $\mathcal{H}_0$ and $\mathcal{H}_1$. Then the density of the observations under $\mathcal{H}_i$, $i \in \{0, 1\}$, is given by

$$p(\boldsymbol{Y} \mid \mathcal{H}_i) = \left[\frac{1}{(\pi\sigma^2)^M}\exp\left[-\frac{1}{\sigma^2}\operatorname{Tr}\left(\hat{\boldsymbol{R}}_i\right)\right]\right]^N. \tag{2}$$

B. Generalized Likelihood Ratio

Due to the presence of unknown parameters, the hypothesis test for this problem is composite and, consequently, no detector exists, in general, which is optimal in the Neyman-Pearson sense for all values of the unknown parameters (that is, uniformly most powerful) [11], [15]. However, decision schemes with acceptably good detection performance may be typically found using well-known rules such as the Generalized Likelihood Ratio (GLR) test [11], [15], [16]. If $\mathcal{L}(\boldsymbol{Y})$ denotes the GLR statistic, under this approach we must decide $\mathcal{H}_1$ when $\mathcal{L}(\boldsymbol{Y}) > \gamma$ and $\mathcal{H}_0$ when $\mathcal{L}(\boldsymbol{Y}) \leq \gamma$, where γ is a threshold set in advance to satisfy a certain probability of false alarm[4]. The GLR statistic is the result of substituting the Maximum Likelihood (ML) estimates of the unknown parameters in the likelihood ratio. In our problem, this operation results in the following statistic:

$$\mathcal{L}(\boldsymbol{Y}) \doteq \frac{\max\limits_{\sigma^2, \boldsymbol{Q}} p(\boldsymbol{Y}; \sigma^2, \boldsymbol{Q} \mid \mathcal{H}_1)}{\max\limits_{\sigma^2} p(\boldsymbol{Y}; \sigma^2 \mid \mathcal{H}_0)}. \tag{3}$$

Under either $\mathcal{H}_0$ or $\mathcal{H}_1$, it is readily found (see e.g. [35, Lemma 3.2.2]) that the value of σ^2 maximizing (2) is

$$\hat{\sigma}_i^2 = \frac{1}{M}\operatorname{Tr}\left(\hat{\boldsymbol{R}}_i\right), \quad i = 0, 1. \tag{4}$$

Substituting (4) in (2) yields

$$p(\boldsymbol{Y}; \hat{\sigma}_i^2 \mid \mathcal{H}_i) = \left[\pi e \cdot \operatorname{Tr}\left(\hat{\boldsymbol{R}}_i\right)\right]^{-MN}.$$

so that the test statistic in (3) becomes

$$\mathcal{L}(\boldsymbol{Y}) = \left[\frac{\operatorname{Tr}\left(\hat{\boldsymbol{R}}_0\right)}{\min\limits_{\boldsymbol{Q}} \operatorname{Tr}\left(\hat{\boldsymbol{R}}_1(\boldsymbol{Q})\right)}\right]^{MN} \tag{5}$$

The rest of the paper addresses the minimization of $\operatorname{Tr}\left(\hat{\boldsymbol{R}}_1(\boldsymbol{Q})\right)$ under several models for $\boldsymbol{Q}$ which incorporate different degrees of prior information, thus determining the feasible set of such optimization problems.

III. Multiantenna detection of BL signals

Let us assume that the transmitted signal has a known bandwidth $\mathcal{B}$, measured in radians per sample. In the case of WM signals, we know that

$$\mathcal{B} = \frac{2\pi \cdot 200 \text{ kHz}}{f_s}. \tag{6}$$

The central frequency ω_c is not known, but it is assumed to belong in a finite set Ω_c of candidate central frequencies. For WM signals, this set is given by

$$\Omega_c = \left\{\frac{2\pi f_k}{f_s},\ k = 0, 1, \ldots, k_{\max}\right\}, \tag{7}$$

where $f_k \doteq f_e + k \cdot 25$ kHz for f_e the minimum carrier frequency, which is related to the edge of the TV channel [31]. For the sake of clarity, we start by considering the case where this set has only one element, i.e., its cardinality $|\Omega_c|$ equals one, so that ω_c can be regarded as known. The case $|\Omega_c| > 1$ will be discussed in Sec. VI-B.

Let us particularize (5) to the BL case by noting that

$$\operatorname{Tr}\left(\hat{\boldsymbol{R}}_1(\boldsymbol{Q})\right) = \frac{1}{N}\sum_{n=0}^{N-1} ||\ \boldsymbol{y}[n] - \boldsymbol{q}[n]\ ||^2, \tag{8}$$

where $\boldsymbol{y}[n]$ and $\boldsymbol{q}[n]$ denote, respectively, the n-th column in $\boldsymbol{Y}$ and $\boldsymbol{Q}$. By virtue of Parseval's identity,

$$\operatorname{Tr}\left(\hat{\boldsymbol{R}}_1(\boldsymbol{Q})\right) = \frac{1}{N^2}\sum_{k=0}^{N-1} ||\tilde{\boldsymbol{y}}(e^{j\omega_k}) - \tilde{\boldsymbol{q}}(e^{j\omega_k})||^2, \tag{9}$$

[3] We conjugate the signal component $x^*[n]$ for notational convenience.

[4] The probability of false alarm (P_{FA}) is defined as the probability of deciding $\mathcal{H}_1$ when $\mathcal{H}_0$ is true.

where $\omega_k \doteq \frac{2\pi}{N}k$ and the DFT vectors $\tilde{\boldsymbol{y}}(e^{j\omega_k})$ and $\tilde{\boldsymbol{q}}(e^{j\omega_k})$ are given by

$$\tilde{\boldsymbol{y}}(e^{j\omega_k}) \doteq \sum_{n=0}^{N-1} \boldsymbol{y}[n]e^{-j\omega_k n},\ \tilde{\boldsymbol{q}}(e^{j\omega_k}) \doteq \sum_{n=0}^{N-1} \boldsymbol{q}[n]e^{-j\omega_k n}.$$

Let us assume, without loss of generality[5], that the frequency support of $x^*[n]$, and therefore that of $\boldsymbol{q}[n]$ as well, spans the first B DFT coefficients[6] ($B = \frac{N}{2\pi}\mathcal{B}$). Then (9) can be written as the sum of two terms as follows:

$$\begin{aligned}\mathrm{Tr}\left(\hat{\boldsymbol{R}}_1(\boldsymbol{Q})\right) = \frac{1}{N^2}\sum_{k=0}^{B-1} ||\tilde{\boldsymbol{y}}(e^{j\omega_k}) - \tilde{\boldsymbol{q}}(e^{j\omega_k})||^2 \\ + \frac{1}{N^2}\sum_{k=B}^{N-1} ||\tilde{\boldsymbol{y}}(e^{j\omega_k})||^2. \quad (10)\end{aligned}$$

Note that only the first term in the right-hand side of (10) depends on $\boldsymbol{Q}$. The rest of this section is devoted to addressing the minimization of this term under two scenarios. First, an arbitrary channel impulse response $\boldsymbol{h}[n]$ is assumed, which means that the signal term $\boldsymbol{q}[n]$ is unstructured. This will result in the simplest of the proposed detectors, which only exploits the BL property. Later, a frequency-flat channel assumption will lead to a rank-1 spatial structure, resulting in a second detector with better performance but higher complexity.

A. Arbitrary Channel Structure

Applying Parseval's identity again to the first term of the right hand side of (10) results in

$$\begin{aligned}\frac{1}{N^2}\sum_{k=0}^{B-1} ||\tilde{\boldsymbol{y}}(e^{j\omega_k}) - \tilde{\boldsymbol{q}}(e^{j\omega_k})||^2 = \\ \frac{1}{N}\sum_{n=0}^{N-1} ||\ \boldsymbol{y}_f[n] - x^*[n] \star \boldsymbol{h}[n]\ ||^2, \quad (11)\end{aligned}$$

where $\boldsymbol{y}_f[n]$ represents a filtered version of $\boldsymbol{y}[n]$ obtained by setting to zero all out-of-band DFT coefficients, i.e.,

$$\boldsymbol{y}_f[n] \doteq \frac{1}{N}\sum_{k=0}^{B-1} \tilde{\boldsymbol{y}}(e^{j\omega_k})e^{j\omega_k n}. \quad (12)$$

Clearly, expression (11), and consequently (10), are minimized when $\boldsymbol{y}_f[n] = x^*[n] \star \boldsymbol{h}[n]$. Since no structure about $\boldsymbol{h}[n]$ or $x^*[n]$ is assumed, it is possible to select their values to satisfy this condition. For example, take $x^*[n]$ as the impulse response of an ideal[7] bandpass filter with passband $\mathcal{B}$, and then pick $\boldsymbol{h}[n] = \boldsymbol{y}_f[n]$. Since $\boldsymbol{y}_f[n]$ is bandlimited to $\mathcal{B}$, it is clear that this choice results in $x^*[n] \star \boldsymbol{h}[n] = x^*[n] \star \boldsymbol{y}_f[n] = \boldsymbol{y}_f[n]$. Consequently, (10) becomes

$$\begin{aligned}\mathrm{Tr}\left(\hat{\boldsymbol{R}}_1(\boldsymbol{Q})\right) &= \frac{1}{N^2}\sum_{k=B}^{N-1} ||\tilde{\boldsymbol{y}}(e^{j\omega_k})||^2 \\ &= \frac{1}{N^2}\sum_{k=0}^{N-1} ||\tilde{\boldsymbol{y}}(e^{j\omega_k})||^2 - \frac{1}{N^2}\sum_{k=0}^{B-1} ||\tilde{\boldsymbol{y}}(e^{j\omega_k})||^2,\end{aligned}$$

or, in the time domain,

$$\mathrm{Tr}\left(\hat{\boldsymbol{R}}_1(\hat{\boldsymbol{Q}})\right) = \frac{1}{N}\sum_{n=0}^{N-1} ||\boldsymbol{y}[n]||^2 - \frac{1}{N}\sum_{n=0}^{N-1} ||\boldsymbol{y}_f[n]||^2. \quad (13)$$

Similarly to $\boldsymbol{Y}$ and $\hat{\boldsymbol{R}}_0$, one can define

$$\boldsymbol{Y}_f \doteq \left[\ \boldsymbol{y}_f[0] \quad \boldsymbol{y}_f[1] \quad \cdots \quad \boldsymbol{y}_f[N-1]\ \right], \quad (14)$$

$$\hat{\boldsymbol{R}}_0^f \doteq \frac{1}{N}\boldsymbol{Y}_f\boldsymbol{Y}_f^H. \quad (15)$$

In that case, (13) becomes $\mathrm{Tr}(\hat{\boldsymbol{R}}_1(\hat{\boldsymbol{Q}})) = \mathrm{Tr}(\hat{\boldsymbol{R}}_0) - \mathrm{Tr}(\hat{\boldsymbol{R}}_0^f)$, so that (5) reduces to

$$\mathcal{L}_{\mathrm{BL}}(\boldsymbol{Y}) = \left[\frac{\mathrm{Tr}\left(\hat{\boldsymbol{R}}_0\right)}{\mathrm{Tr}\left(\hat{\boldsymbol{R}}_0\right) - \mathrm{Tr}\left(\hat{\boldsymbol{R}}_0^f\right)}\right]^{MN}. \quad (16)$$

Since two tests statistics related by a one-to-one transformation define the same test as long as the decision regions are properly set [11], [15], testing $\mathcal{L}_{\mathrm{BL}}(\boldsymbol{Y})$ in (16) amounts to testing

$$T_{\mathrm{BL}}(\boldsymbol{Y}) = \frac{\mathrm{Tr}\left(\hat{\boldsymbol{R}}_0^f\right)}{\mathrm{Tr}\left(\hat{\boldsymbol{R}}_0\right)} = \frac{||\boldsymbol{Y}_f||_F^2}{||\boldsymbol{Y}||_F^2}. \quad (17)$$

Henceforth we will refer to (17) as the bandlimited detector (BL), since this is the only property it exploits. Note that it just measures the ratio of the in-band energy to the total energy.

B. Frequency-Flat Channels

As the WM signal is narrowband relative to the operational bandwidth, the channel response can be regarded as frequency-flat. This results in a rank-1 structure for $\boldsymbol{Q}$, i.e., $\boldsymbol{Q} = \boldsymbol{h}\boldsymbol{x}^H$, where $\boldsymbol{h}$ contains the channel coefficients and $\boldsymbol{x}^H \doteq [x^*[-n_0], x^*[-n_0+1], \cdots, x^*[N-n_0-1]]$. This reads in the frequency domain as $\tilde{\boldsymbol{q}}(e^{j\omega_k}) = \tilde{x}^*(e^{-j\omega_k})\boldsymbol{h}$, where $\tilde{x}(e^{j\omega_k}) \doteq \sum_{n=0}^{N-1} x[n]e^{-j\omega_k n}$. Therefore, optimizing w.r.t. $\boldsymbol{Q}$ amounts to optimizing w.r.t. $\tilde{x}(e^{j\omega_k})$ and $\boldsymbol{h}$. We first find the minimum of

$$||\tilde{\boldsymbol{y}}(e^{j\omega_k}) - \tilde{\boldsymbol{q}}(e^{j\omega_k})||^2 = ||\tilde{\boldsymbol{y}}(e^{j\omega_k}) - \tilde{x}^*(e^{-j\omega_k})\boldsymbol{h}||^2 \quad (18)$$

w.r.t. $\tilde{x}(e^{j\omega_k})$ for each ω_k with $k = 0,\ldots, B-1$. This is a typical least squares (LS) problem, whose solution is given by

$$\begin{aligned}\min_{\tilde{x}(e^{j\omega_k})} ||\tilde{\boldsymbol{y}}(e^{j\omega_k}) - \tilde{x}^*(e^{-j\omega_k})\boldsymbol{h}||^2 \\ = ||\tilde{\boldsymbol{y}}(e^{j\omega_k})||^2 - \frac{|\boldsymbol{h}^H\tilde{\boldsymbol{y}}(e^{j\omega_k})|^2}{||\boldsymbol{h}||^2}. \quad (19)\end{aligned}$$

[5]The reason is that the detection problem is invariant [15] to modulating the signals received at all antennas by the same complex exponential, which may have an arbitrary frequency.

[6]Strictly speaking, the observed signal is only approximately bandlimited, since we observe a finite number of samples N. Nevertheless, throughout the paper it is assumed that N is sufficiently large, so that the windowing effects can be neglected and the signal can be regarded as truly bandlimited. This is justified by the fact that, in practice, stringent low-SNR detectability requirements cannot be met with small values of N.

[7]A rigorous proof can be provided without resorting to ideal filters, but it is omitted due to space limitations.

Substituting (19) in (10) yields

$$\mathrm{Tr}\left(\hat{\boldsymbol{R}}_1(\boldsymbol{h})\right) = \frac{1}{N^2}\sum_{k=0}^{N-1}||\tilde{\boldsymbol{y}}(e^{j\omega_k})||^2 - \frac{1}{N^2}\sum_{k=0}^{B-1}\frac{|\boldsymbol{h}^H\tilde{\boldsymbol{y}}(e^{j\omega_k})|^2}{||\boldsymbol{h}||^2}. \quad (20)$$

Applying Parseval's identity results in

$$\begin{aligned}\mathrm{Tr}\left(\hat{\boldsymbol{R}}_1(\boldsymbol{h})\right) &= \frac{1}{N}\sum_{n=0}^{N-1}||\boldsymbol{y}[n]||^2 - \frac{1}{N}\frac{||\boldsymbol{h}^H\boldsymbol{Y}_f||^2}{||\boldsymbol{h}||^2} \\ &= \mathrm{Tr}\left(\hat{\boldsymbol{R}}_0\right) - \frac{\boldsymbol{h}^H\hat{\boldsymbol{R}}_0^f\boldsymbol{h}}{||\boldsymbol{h}||^2}. \quad (21)\end{aligned}$$

The vector $\boldsymbol{h}$ minimizing (21) is given by the principal eigenvector of $\hat{\boldsymbol{R}}_0^f$. Hence,

$$\min_{\boldsymbol{h}}\ \mathrm{Tr}\left(\hat{\boldsymbol{R}}_1(\boldsymbol{h})\right) = \mathrm{Tr}\left(\hat{\boldsymbol{R}}_0\right) - \lambda_1\left(\hat{\boldsymbol{R}}_0^f\right), \quad (22)$$

where $\lambda_1(\boldsymbol{A})$ denotes the largest eigenvalue of $\boldsymbol{A}$. Substituting (22) into (5) yields

$$\mathcal{L}_{\text{BLFF}}(\boldsymbol{Y}) = \left[\frac{\mathrm{Tr}\left(\hat{\boldsymbol{R}}_0\right)}{\mathrm{Tr}\left(\hat{\boldsymbol{R}}_0\right) - \lambda_1\left(\hat{\boldsymbol{R}}_0^f\right)}\right]^{MN}.$$

For detection purposes, this statistic is equivalent to

$$T_{\text{BLFF}}(\boldsymbol{Y}) = \frac{\lambda_1\left(\hat{\boldsymbol{R}}_0^f\right)}{\mathrm{Tr}\left(\hat{\boldsymbol{R}}_0\right)} = \frac{||\boldsymbol{Y}_f||_{2,2}^2}{||\boldsymbol{Y}||_F^2}. \quad (23)$$

Henceforth, we will refer to the test defined by this statistic as the Bandlimited Frequency-Flat detector (BLFF). Observe that (23) reduces to the well-known multiantenna "λ_1/trace" detector [10], [23], [25] when the signal is not bandlimited, i.e., when $B = N$, since in that case the only property this detector can exploit is the spatial structure.

IV. Multiantenna detection of CM signals

In this section we derive the GLR test which only exploits the CM property of the WM signal. We minimize $\mathrm{Tr}(\hat{\boldsymbol{R}}_1(\boldsymbol{Q}))$ assuming that the transmitted signal $x[n]$ has this property, although it may not be bandlimited. As it turns out, the existence of the GLR depends on whether the frequency-flat assumption on the channel applies or not.

A. Arbitrary Channel Structure

From expression (8), it is possible to write

$$\mathrm{Tr}\left(\hat{\boldsymbol{R}}_1(\boldsymbol{Q})\right) = \frac{1}{N}\sum_{n=0}^{N-1}||\ \boldsymbol{y}[n] - x^*[n]\star\boldsymbol{h}[n]\ ||^2. \quad (24)$$

Due again to the fact that no structure is imposed on $\boldsymbol{h}[n]$, it follows that (24) can be made zero: for example, pick $x^*[n]$ as any CM signal with no spectral zeros, and choose each entry of $\boldsymbol{h}[n]$ as the signal whose spectrum equals that of the corresponding entry of $\boldsymbol{y}[n]$ divided by the spectrum of $x^\star[n]$. This results in $x^*[n]\star\boldsymbol{h}[n] = \boldsymbol{y}[n]$, so that (24) vanishes. As a result, the denominator in (5) vanishes and no GLR is defined for this case. This makes sense, since the CM property of the transmitted signal, which is the only signal feature that can be exploited for detection purposes in this case, is wiped out after passing through a frequency-selective channel.

B. Frequency-Flat Channels

Assume now that the channel is frequency flat. As seen in Sec. III-B, in that case the matrix $\boldsymbol{Q}$ is rank-1, i.e., $\boldsymbol{Q} = \boldsymbol{h}\boldsymbol{x}^H$. In order to make explicit the CM property of the transmitted signal, let us denote it as $\boldsymbol{x}(\boldsymbol{\phi}) \doteq [e^{j\phi_0}\ e^{j\phi_1}\ \ldots\ e^{j\phi_{N-1}}]^T$, where $\boldsymbol{\phi} \doteq [\phi_0\ \phi_1\ \ldots\ \phi_{N-1}]^T$. Note that there is no loss of generality in assuming unit magnitude, since any scaling factor can be absorbed by the channel vector $\boldsymbol{h}$. Then,

$$\begin{aligned}\mathrm{Tr}\left(\hat{\boldsymbol{R}}_1(\boldsymbol{h},\boldsymbol{\phi})\right) = \frac{1}{N}[&\mathrm{Tr}\left(\boldsymbol{Y}\boldsymbol{Y}^H\right) \quad (25)\\ &- 2\,\mathrm{Re}\left\{\boldsymbol{h}^H\boldsymbol{Y}\boldsymbol{x}(\boldsymbol{\phi})\right\} + N||\boldsymbol{h}||^2],\end{aligned}$$

since $\boldsymbol{x}^H(\boldsymbol{\phi})\boldsymbol{x}(\boldsymbol{\phi}) = N$. The ML estimate of $\boldsymbol{\phi}$ is given by

$$\begin{aligned}\hat{\boldsymbol{\phi}} &= \arg\max_{\boldsymbol{\phi}}\ \mathrm{Re}\left\{\boldsymbol{h}^H\boldsymbol{Y}\boldsymbol{x}(\boldsymbol{\phi})\right\} \quad (26)\\ &= \arg\max_{\boldsymbol{\phi}}\mathrm{Re}\left\{\sum_{n=0}^{N-1}e^{j\phi_n}\boldsymbol{h}^H\boldsymbol{y}[n]\right\}, \quad (27)\end{aligned}$$

which results in $\hat{\phi}_n = -\angle\left(\boldsymbol{h}^H\boldsymbol{y}[n]\right)$. The optimal value is therefore $\sum_n|\boldsymbol{h}^H\boldsymbol{y}[n]| = ||\boldsymbol{Y}^H\boldsymbol{h}||_1$. Substituting this back in (25) gives

$$\mathrm{Tr}\left(\hat{\boldsymbol{R}}_1(\boldsymbol{h},\hat{\boldsymbol{\phi}})\right) = \frac{1}{N}\left[\mathrm{Tr}\left(\boldsymbol{Y}\boldsymbol{Y}^H\right) - 2||\boldsymbol{Y}^H\boldsymbol{h}||_1 + N||\boldsymbol{h}||^2\right]. \quad (28)$$

In order to minimize this expression w.r.t. $\boldsymbol{h}$, write $\boldsymbol{h} = \rho\cdot\boldsymbol{g}$, with $\rho > 0$ and $||\boldsymbol{g}|| = 1$. The optimal value of ρ is readily found to be $\hat{\rho} = \frac{1}{N}||\boldsymbol{Y}^H\boldsymbol{g}||_1$. Using this expression, the ML estimate of the spherical component $\boldsymbol{g}$ is seen to be

$$\hat{\boldsymbol{g}} = \arg\max_{\boldsymbol{g}}||\boldsymbol{Y}^H\boldsymbol{g}||_1 \quad \text{s.t.}\ \ ||\boldsymbol{g}|| = 1. \quad (29)$$

The solution to this problem, $||\boldsymbol{Y}^H||_{2,1} \doteq ||\boldsymbol{Y}^H\hat{\boldsymbol{g}}||_1$ is known as the *operator norm*, *dual norm*, or *subordinate norm* to the vector ℓ^2- and ℓ^1-norms [36]–[39]. An iterative method for solving this constrained optimization problem is presented in the Appendix. Substituting this solution produces

$$\mathrm{Tr}\left(\hat{\boldsymbol{R}}_1(\hat{\boldsymbol{h}},\hat{\boldsymbol{\phi}})\right) = \frac{1}{N}\left[||\boldsymbol{Y}||_F^2 - \frac{1}{N}||\boldsymbol{Y}^H||_{2,1}^2\right]. \quad (30)$$

Finally, using (30) in (5) gives

$$\mathcal{L}_{\text{CM}}(\boldsymbol{Y}) = \left[\frac{||\boldsymbol{Y}||_F^2}{||\boldsymbol{Y}||_F^2 - \frac{1}{N}||\boldsymbol{Y}^H||_{2,1}^2}\right]^{MN}, \quad (31)$$

which is a monotonically increasing function of the equivalent test statistic

$$T_{\text{CM}}(\boldsymbol{Y}) = \frac{||\boldsymbol{Y}^H||_{2,1}^2}{||\boldsymbol{Y}||_F^2}. \quad (32)$$

The detector defined by (32) will be referred to as the CM detector, since it exploits the CM property. Although it also exploits the rank-1 structure of the signal term, we will dismiss this fact in the notation since, as seen in Sec. IV-A, no GLR detector exists that exploits the CM property for arbitrary channel structure.

V. Detection of CM bandlimited signals

We consider now the complete model capturing the entire prior knowledge about the WM signal. Regarding the minimization of $\mathrm{Tr}\left(\hat{\boldsymbol{R}}_1(\boldsymbol{Q})\right)$, it can be readily shown, analogously to Sec. IV-A, that if an arbitrary channel impulse response is assumed, then the CM constraint on the signal still allows to make zero the signal term within the frequency support of the transmitted signal. However, in this case the denominator of (5) does not vanish because of the contribution of the out-of-band noise, thus resulting in a well-defined GLR statistic. The resulting test turns out to be equivalent to the BL detector in (17). This is consistent with our findings in Sec. IV-A: since the passage of a CM signal through a frequency selective channel destroys the CM property at the channel output, it is reasonable that the corresponding detector cannot exploit such property. However, the situation is different with frequency-flat channels, as discussed next.

Let us start by noting that the fact that the signal is bandlimited allows us to write the trace of the sample covariance matrix again as in (10). However, the optimization w.r.t. $\tilde{\boldsymbol{q}}(e^{j\omega_k})$ now has to take into account the CM feature, which is a time-domain property. As we will see, a solution can be found by confining ourselves to the frequency support of $\tilde{\boldsymbol{q}}(e^{j\omega_k})$.

As seen in Sec. III-A, for frequency-flat channels it holds that $\tilde{\boldsymbol{q}}(e^{j\omega_k}) = \tilde{x}^*(e^{-j\omega_k})\boldsymbol{h}$, so that we can rewrite the first term in the right-hand side of (10) as

$$\begin{aligned}\frac{1}{N^2}\sum_{k=0}^{B-1}||\tilde{\boldsymbol{y}}(e^{j\omega_k}) - \tilde{\boldsymbol{q}}(e^{j\omega_k})||^2 \qquad (33)\\ = \frac{1}{N^2}\sum_{k=0}^{B-1}||\tilde{\boldsymbol{y}}(e^{j\omega_k}) - \tilde{x}^*(e^{-j\omega_k})\boldsymbol{h}||^2.\end{aligned}$$

Now let $L \doteq N/B$. For a signal $z[n]$, let $z_d[n]$ denote the signal obtained by ideally[8] bandpass filtering $z[n]$ to the interval $[0, 2\pi/L]$ followed by a downsampling operation[9] with a factor L (see, e.g., [40]). Then one has $\tilde{z}(e^{j\omega}) = L\cdot\tilde{z}_d(e^{j\omega L})$ for $\omega \in [0, 2\pi/L]$. It follows that (33) can be written as

$$\begin{aligned}&\frac{1}{N^2}\sum_{k=0}^{B-1}||\tilde{\boldsymbol{y}}(e^{j\omega_k}) - \tilde{\boldsymbol{q}}(e^{j\omega_k})||^2\\ &\quad= \frac{L^2}{N^2}\sum_{k=0}^{B-1}||\tilde{\boldsymbol{y}}_d(e^{j\frac{2\pi kL}{N}}) - \tilde{x}_d^*(e^{-j\frac{2\pi kL}{N}})\boldsymbol{h}||^2 \qquad (34)\\ &\quad= \frac{1}{B}\sum_{n=0}^{B-1}||\boldsymbol{y}_d[n] - x_d^*[n]\boldsymbol{h}||^2 \qquad (35)\\ &\quad= \mathrm{Tr}\left(\hat{\boldsymbol{R}}_1^d(\boldsymbol{h}, \boldsymbol{x}_d)\right), \qquad (36)\end{aligned}$$

where in (35) we have applied Parseval's identity (note that the sequences $\boldsymbol{y}_d[n]$, $x_d[n]$ have length $N/L = B$), whereas in (36) we have introduced the matrix

$$\hat{\boldsymbol{R}}_1^d \doteq \frac{1}{B}\left(\boldsymbol{Y}_d - \boldsymbol{h}\boldsymbol{x}_d^H\right)\left(\boldsymbol{Y}_d - \boldsymbol{h}\boldsymbol{x}_d^H\right)^H \in \mathbb{C}^{M\times M}, \qquad (37)$$

with

$$\boldsymbol{Y}_d \doteq \left[\begin{array}{cccc}\boldsymbol{y}_d[0] & \boldsymbol{y}_d[1] & \cdots & \boldsymbol{y}_d[B-1]\end{array}\right] \in \mathbb{C}^{M\times B}, \qquad (38)$$

$$\boldsymbol{x}_d \doteq \left[\begin{array}{cccc}x_d[0] & x_d[1] & \cdots & x_d[B-1]\end{array}\right]^T \in \mathbb{C}^{B}. \qquad (39)$$

Note now that minimizing (36) w.r.t. $\boldsymbol{h}$ and $\boldsymbol{x}_d$ subject to the CM constraint on $\boldsymbol{x}_d$ (since the decimation operation by an arbitrary factor preserves the CM property of a signal) is a problem analogous to that found in Sec. IV-B. Therefore, the same approach can be applied, resulting in the following minimum value for (36):

$$\mathrm{Tr}\left(\hat{\boldsymbol{R}}_1^d(\hat{\boldsymbol{h}}, \hat{\boldsymbol{x}}_d)\right) = \frac{1}{B}\left[\mathrm{Tr}\left(\boldsymbol{Y}_d\boldsymbol{Y}_d^H\right) - \frac{1}{B}||\boldsymbol{Y}_d^H||_{2,1}^2\right]. \qquad (40)$$

Substituting (40) back in (10) yields

$$\begin{aligned}\mathrm{Tr}\left(\hat{\boldsymbol{R}}_1(\boldsymbol{Q})\right) = \frac{1}{B}\left[\mathrm{Tr}\left(\boldsymbol{Y}_d\boldsymbol{Y}_d^H\right) - \frac{1}{B}||\boldsymbol{Y}_d^H||_{2,1}^2\right]\\ + \frac{1}{N}\mathrm{Tr}\left(\boldsymbol{Y}\boldsymbol{Y}^H\right) - \frac{1}{N}\mathrm{Tr}\left(\boldsymbol{Y}_f\boldsymbol{Y}_f^H\right),\end{aligned}$$

with $\boldsymbol{Y}_f$ the filtered data matrix given by (14). Hence, the expression for the GLR statistic is

$$\mathcal{L}_{\text{CMBL}}(\boldsymbol{Y}) = \left[\frac{||\boldsymbol{Y}||_F^2}{L\left(||\boldsymbol{Y}_d||_F^2 - \frac{1}{B}||\boldsymbol{Y}_d^H||_{2,1}^2\right) + ||\boldsymbol{Y}||_F^2 - ||\boldsymbol{Y}_f||_F^2}\right]^{MN} \qquad (41)$$

This detector will be referred to as the CM Bandlimited detector (CMBL), and exploits the whole prior information about WM signals. Thus, it is expected to offer the best performance of all the detectors presented in this paper, although it is at the expense of presenting the highest computational complexity.

VI. Remarks

A. Interpretation

All the GLRs derived for bandlimited signals in previous sections have the same general form; namely, all of them can be written as

$$\mathcal{L}(\boldsymbol{Y}) = \left[\frac{\hat{\sigma}^2_{\text{tot}}}{\hat{\sigma}^2_{\text{in}} + \hat{\sigma}^2_{\text{out}}}\right]^{MN}, \qquad (42)$$

where $\hat{\sigma}^2_{\text{tot}} = \mathrm{Tr}(\hat{\boldsymbol{R}}_0)$ is an estimate of the total power of the observations, whereas $\hat{\sigma}^2_{\text{in}}$ and $\hat{\sigma}^2_{\text{out}}$ are, respectively, estimates of the in-band and out-of-band *noise* powers.

An alternative form, which was already used in (17) and (23), follows from noting that an estimate of the in-band signal power can be obtained as $\hat{s}^2 = \hat{\sigma}^2_{\text{tot}} - (\hat{\sigma}^2_{\text{in}} + \hat{\sigma}^2_{\text{out}})$. This allows to rewrite (42) as $\mathcal{L}(\boldsymbol{Y}) = \left[\sigma^2_{\text{tot}}/(\hat{\sigma}^2_{\text{tot}} - \hat{s}^2)\right]^{MN}$, leading to the equivalent statistic $T(\boldsymbol{Y}) = \hat{s}^2/\hat{\sigma}^2_{\text{tot}}$. The proposed detectors are seen to use different in-band signal power estimates:

- For the BL detector, one has $\hat{s}^2 = \mathrm{Tr}\left(\hat{\boldsymbol{R}}_0^f\right)$, i.e., all of the in-band power is ascribed to the signal component, so that $\hat{\sigma}^2_{\text{in}} = 0$.
- For the BLFF detector, one has $\hat{s}^2 = \lambda_1\left(\hat{\boldsymbol{R}}_0^f\right)$, which is an estimator of the power in the principal eigenspace of the filtered covariance matrix. The prior information

[8]Note that some performance degradation may be expected in practice due to the usage of non-ideal filters.

[9]Note that L may not be, in general, an integer number, so that a previous interpolation step may be required.

being exploited here is the rank-1 property of the signal subspace.

- For the CMBL detector, inspection of the denominator in (41) shows that $\hat{s}^2 = \|\boldsymbol{Y}_f\|_F^2 - L\|\boldsymbol{Y}_d\|_F^2 + LB^{-1}\|\boldsymbol{Y}_d^H\|_{2,1}^2$. For large N, the energy of the downsampled sequence $\boldsymbol{y}_d[n]$ relates to that of the filtered sequence $\boldsymbol{y}_f[n]$ as $\|\boldsymbol{Y}_d\|_F^2 \approx \frac{1}{L}\|\boldsymbol{Y}_f\|_F^2$ [40], and therefore $\hat{s}^2 \approx LB^{-1}\|\boldsymbol{Y}_d^H\|_{2,1}^2$. This observation suggests the following modification of the test statistic (41):

$$\mathcal{L}_{\text{CMBL}}(\boldsymbol{Y}) \approx \left[\frac{||\boldsymbol{Y}||_F^2}{||\boldsymbol{Y}||_F^2 - \frac{L}{B}||\boldsymbol{Y}_d^H||_{2,1}^2}\right]^{MN}, \qquad (43)$$

which, for detection purposes, is equivalent to the statistic

$$T_{\text{CMBL}}(\boldsymbol{Y}) = \frac{||\boldsymbol{Y}_d^H||_{2,1}^2}{||\boldsymbol{Y}||_F^2}. \qquad (44)$$

Clearly, the statistic in (44) has a lower computational complexity than that in (41). Moreover, empirical results reveal that this asymptotic (large N) version of the CMBL test significantly improves the detection performance with respect to that of the original formulation (41) and reduces the influence of the particular choice of the filters. Note that (44) reduces to (32) when the BL assumption is dropped, since in that case one has $\boldsymbol{Y}_d = \boldsymbol{Y}$.

B. Dealing with an unknown carrier frequency

In practice, the carrier frequency of the WM signal is not known and, therefore, using certain GLR detectors involves maximizing the corresponding statistic w.r.t. this carrier frequency parameter ω_c over the set Ω_c of candidate values, as in [19]. From (7), the number of candidate carrier frequencies $|\Omega_c|$ in a 6 MHz TV channel is 237. Since $|\Omega_c|$ has a dominant impact on the computational complexity of some of the proposed detectors (see Sec. VI-D), it is convenient to devise a method to set $|\Omega_c|$ somewhere in between 0 and 237 to trade performance for complexity.

In this respect, the detectors proposed in this paper present an important advantage over previous schemes from the literature, e.g. [19]: since the carrier frequency is not explicitly used by the detector, it is possible to divide the 6 MHz channel in a reduced number of overlapping intervals with bandwidth larger than 200 kHz. This operation reduces $|\Omega_c|$ and increases the bandwidth of each segment $\mathcal{B}$, which allows for a significant reduction in computational complexity in exchange for some degradation in performance. Interestingly, as will be seen in Sec. VIII, the loss incurred by this approach is small provided that the number of subbands is large enough.

We also remark that some of the proposed detectors allow certain simplifications when performing a series of evaluations for different central frequencies $\omega_c \in \Omega_c$. Consider first the case of the BL statistic (17), for which one must compute

$$\text{Tr}\left(\hat{\boldsymbol{R}}_0^f\right) = \frac{1}{N^2}\sum_{k=0}^{N-1} p_k(\omega_c)||\tilde{\boldsymbol{y}}(e^{j\frac{2\pi k}{N}})||^2 \qquad (45)$$

for all $\omega_c \in \Omega_c$, where $p_k(\omega_c)$ denotes the frequency response of the bandpass filter, i.e., $p_k(\omega_c) = 1$ for the B bins centered at ω_c and zero otherwise. Thus, it suffices to compute the DFT of the observations and then store the squared magnitudes $||\tilde{\boldsymbol{y}}(e^{j\frac{2\pi k}{N}})||^2$; after that, only $B-1$ additions per candidate central frequency are required.

Regarding the BLFF statistic (23), it is seen that $\lambda_1(\hat{\boldsymbol{R}}_0^f)$ must be computed for each ω_c. To this end, let $\boldsymbol{F} \in \mathbb{C}^{N\times N}$ be the Fourier matrix, so that $\tilde{\boldsymbol{u}}^T = \boldsymbol{u}^T\boldsymbol{F}$ is the DFT of the row vector $\boldsymbol{u}^T$. Note that $\boldsymbol{F}^H\boldsymbol{F} = \boldsymbol{F}\boldsymbol{F}^H = N\boldsymbol{I}$. Then $\tilde{\boldsymbol{Y}} = \boldsymbol{Y}\boldsymbol{F}$ is the DFT of the observations, and one has $\boldsymbol{Y}_f = \frac{1}{N}\tilde{\boldsymbol{Y}}\boldsymbol{P}(\omega_c)\boldsymbol{F}^H$, where $\boldsymbol{P}(\omega_c) \doteq \text{diag}\{p_0(\omega_c), p_1(\omega_c), \cdots, p_{N-1}(\omega_c)\}$. Therefore $\hat{\boldsymbol{R}}_0^f = \frac{1}{N}\boldsymbol{Y}_f\boldsymbol{Y}_f^H = \frac{1}{N^2}\tilde{\boldsymbol{Y}}\boldsymbol{P}(\omega_c)\boldsymbol{P}^H(\omega_c)\tilde{\boldsymbol{Y}}^H$. Since $\lambda_1(\hat{\boldsymbol{R}}_0^f) = \frac{1}{N^2}\lambda_1(\tilde{\boldsymbol{Y}}\boldsymbol{P}(\omega_c)\boldsymbol{P}^H(\omega_c)\tilde{\boldsymbol{Y}}^H) = \frac{1}{N^2}\lambda_1(\boldsymbol{P}^H(\omega_c)\tilde{\boldsymbol{Y}}^H\tilde{\boldsymbol{Y}}\boldsymbol{P}(\omega_c))$, one can compute first the matrix $\tilde{\boldsymbol{Y}}^H\tilde{\boldsymbol{Y}}$, and then, for each $\omega_c \in \Omega_c$, select the suitable rows and columns and evaluate the largest eigenvalue.

Finally, the CMBL statistic (44) requires the computation of $||\boldsymbol{Y}_d^H||_{2,1}^2$ for each $\omega_c \in \Omega_c$. If $L = N/B$ is an integer[10], then $\boldsymbol{Y}_d$ can be directly obtained as $\boldsymbol{Y}_d = \boldsymbol{Y}_f\boldsymbol{S} = \frac{1}{N}\tilde{\boldsymbol{Y}}\boldsymbol{P}(\omega_c)\boldsymbol{F}^H\boldsymbol{S}$, where $\boldsymbol{S} \in \mathbb{C}^{N\times B}$ is a decimation matrix containing the appropriate set of B columns of the $N\times N$ identity matrix. If L is not an integer, but $L = L_1/L_2$ with L_1, L_2 coprime, then $\boldsymbol{Y}_d$ can still be obtained from $\boldsymbol{Y}_f$ by first upsampling by a factor L_2, followed by appropriate bandpass filtering and finally downsampling by a factor L_1. Once $\boldsymbol{Y}_d$ is obtained, the computation of $||\boldsymbol{Y}_d^H||_{2,1}^2$ can be addressed as shown in the Appendix.

C. Interference from TV stations

It has been assumed so far that the sensed channel is in one of two possible states: $\mathcal{H}_1$: *WM signal plus noise* or $\mathcal{H}_0$: *noise only*. The reason is that it was implicitly assumed that a TV signal detector is applied before the detector for WMs, the latter being executed only when the former declares the channel free from TV signals. However, there exists a potential risk that a TV signal is present when the WM detector is applied, which would be a consequence of a miss detection event of the TV detector. It has been observed that the effects of this TV interference on the performance of the WM detectors are mixed: depending on the PSD and direction of arrival of the interference signal, the performance of the WM detector may be improved or degraded. In any case, since a miss detection of the TV detector takes place in cases where the level of the TV signal is well below the background noise, we expect a small influence of this interference on the performance of the WM detectors.

D. Computational complexity

According to what was explained in Sec. VI-B, the BL detector requires the computation of $||\tilde{\boldsymbol{y}}(e^{j\frac{2\pi k}{N}})||^2$ for $k = 0, \ldots, N-1$. This requires M fast Fourier transforms (FFTs), with complexity $O(MN\log N)$, and the computation of N squared magnitudes of vectors in $\mathbb{C}^M$, which is $O(NM)$.

[10]This is the typical case, since for WMs in 6 MHz bands, this factor is $L = 6$ MHz/200 kHz$= 30$.

After that, just a few sums are needed, which means that the complexity of the BL detector is $O(MN \log N)$.

Besides the M FFTs, the BLFF detector requires the computation of $\tilde{\boldsymbol{Y}}^H \tilde{\boldsymbol{Y}}$, which is $O(MN^2)$. Then $|\Omega_c|$ eigenvalues must be computed, for example using the standard power method with I iterations, resulting in a complexity of $O(I|\Omega_c|B^2)$. We therefore conclude that the BLFF detector has complexity $O(\max(I|\Omega_c|B^2, MN^2))$, which is higher than the complexity of the BL detector.

In the case of the CM detector, the complexity is dominated by that of the computation of $||\boldsymbol{Y}^H||_{2,1}$. Using the algorithm proposed in the Appendix with I iterations, it can be seen that this operation is $O(IM^2N)$.

The number of operations required by the CMBL detector is the largest one since the computations must be performed in the time domain. This means that one FFT and $|\Omega_c|$ inverse FFTs (IFFTs) are required, resulting in a complexity of $O(|\Omega_c|MN \log N)$. The execution of the power method requires, in this case, $O(|\Omega_c|IM^2N/B)$ operations, whereas further computations may require up to $O(M^2N)$. Therefore, the complexity of the CMBL detector is $O(|\Omega_c|MN \log N)$.

VII. Performance Analysis

It is important to evaluate the detection performance of the tests presented above so that they can be utilized in practical communication scenarios. Typical characterization of the performance is given in terms of probability of false alarm (P_{FA}), probability of detection[11] (P_{D}) and receiver operating characteristics (ROCs) [11]. The first one affects the capacity of the secondary network whereas the second one determines the interference introduced to the primary network. The ROC curve is used to analyze the trade-off between probability of false alarm and probability of detection. We start by discussing the detectors for bandlimited signals.

A. BL detector

The exact distribution of the BL detector (17) when $|\Omega_c| = 1$ can be obtained as follows. Note from (45) that the BL statistic can be rewritten as

$$T_{\text{BL}}(\boldsymbol{Y}) = \frac{\sum_{k=0}^{N-1} p_k ||\tilde{\boldsymbol{y}}(e^{j\omega_k})||^2}{\sum_{k=0}^{N-1} p_k ||\tilde{\boldsymbol{y}}(e^{j\omega_k})||^2 + \sum_{k=0}^{N-1}(1-p_k)||\tilde{\boldsymbol{y}}(e^{j\omega_k})||^2},$$

where again $p_k = 1$ if the k-th bin is within the passband, and zero otherwise. Hence, this test is equivalent to testing for

$$T'_{\text{BL}}(\boldsymbol{Y}) = \frac{\sum_{k=0}^{N-1} p_k ||\tilde{\boldsymbol{y}}(e^{j\omega_k})||^2}{\sum_{k=0}^{N-1}(1-p_k)||\tilde{\boldsymbol{y}}(e^{j\omega_k})||^2} \tag{46}$$

$$= \frac{\sum_{k=0}^{B-1} ||\tilde{\boldsymbol{y}}(e^{j\omega_k})||^2}{\sum_{k=B}^{N-1} ||\tilde{\boldsymbol{y}}(e^{j\omega_k})||^2}, \tag{47}$$

where in (47) it has been assumed without loss of generality that the passband comprises bins with indices $k = 0, 1, \ldots B-1$. Denote now by $\boldsymbol{w}[n]$ the n-th column of the noise matrix $\boldsymbol{W}$, and let

$$\tilde{\boldsymbol{w}}(e^{j\omega_k}) \doteq \sum_{n=0}^{N-1} \boldsymbol{w}[n] e^{-j\omega_k n}.$$

Then (47) can be rewritten as

$$T'_{\text{BL}}(\boldsymbol{Y}) = \frac{\sum_{k=0}^{B-1} ||\tilde{\boldsymbol{q}}(e^{j\omega_k}) + \tilde{\boldsymbol{w}}(e^{j\omega_k})||^2}{\sum_{k=B}^{N-1} ||\tilde{\boldsymbol{w}}(e^{j\omega_k})||^2}, \tag{48}$$

since $\tilde{\boldsymbol{q}}(e^{j\omega_k}) = \boldsymbol{0}$ for $k \geq B$. The distribution of (48) follows by noting that $\tilde{\boldsymbol{q}}(e^{j\omega_k})$ is deterministic whereas $\tilde{\boldsymbol{w}}(e^{j\omega_k})$ is Gaussian. Hence, the numerator is a scaled non-central χ^2 random variable, whereas the denominator is central χ^2. Thus, $\frac{N-B}{B} T'_{\text{BL}}(\boldsymbol{Y})$ is a non-central Snedecor's F-distributed random variable with non-centrality parameter $\lambda = \frac{2}{N\sigma^2} \sum_k ||\tilde{\boldsymbol{q}}(e^{j\omega_k})||^2 = \frac{2}{\sigma^2} \text{Tr}\left(\boldsymbol{Q}\boldsymbol{Q}^H\right)$ and degrees of freedom $\nu_1 = 2MB$ and $\nu_2 = 2M(N-B)$. Obviously, one has that $\lambda = 0$ under $\mathcal{H}_0$ and $\lambda > 0$ under $\mathcal{H}_1$.

Therefore, if $F_{\lambda,\nu_1,\nu_2}(t)$ denotes the cumulative distribution function corresponding to the F-distribution, it is clear that, once a threshold η is fixed, the probability of false alarm will be given by $P_{\text{FA}} = 1 - F_{0,\nu_1,\nu_2}(\eta)$ whereas the probability of detection will be $P_{\text{D}} = 1 - F_{\lambda,\nu_1,\nu_2}(\eta)$. Combining both expressions results in the receiver operating characteristic: $P_{\text{D}} = 1 - F_{\lambda,\nu_1,\nu_2}(F^{-1}_{0,\nu_1,\nu_2}(1 - P_{\text{FA}}))$. These expressions provide complete characterization of the performance of the BL detector and allows to set the threshold η in order to attain any given P_{FA} or P_{D}.

B. BLFF detector

The evaluation of the distribution of the BLFF statistic turns out to be considerably more involved. Under $\mathcal{H}_0$, by using asymptotic considerations similar to those in [23] we can approximate $\text{Tr}\left(\hat{\boldsymbol{R}}_0\right) \approx M\sigma^2$ for large N, so that (23) becomes

$$T_{\text{BLFF}}(\boldsymbol{Y}) \approx \frac{\lambda_1\left(\boldsymbol{Y}_f \boldsymbol{Y}_f^H\right)}{MN\sigma^2} = \frac{\lambda_1\left(\boldsymbol{Y}_f^H \boldsymbol{Y}_f\right)}{MN\sigma^2}. \tag{49}$$

The test is thus equivalently defined as that deciding $\mathcal{H}_1$ when

$$MN^2 \cdot T_{\text{BLFF}}(\boldsymbol{Y}) = \frac{N}{\sigma^2} \lambda_1\left(\boldsymbol{Y}_f^H \boldsymbol{Y}_f\right) > \gamma, \tag{50}$$

for some threshold γ. In order to compute the probability of false alarm, we note that under $\mathcal{H}_0$ the observations $\boldsymbol{Y}_f$ are the result of filtering white noise through a bandpass filter of bandwidth $\mathcal{B}$. Using the notation introduced in Sec. VI-B, this means that $\boldsymbol{Y}_f = \frac{1}{N}\boldsymbol{Y}\boldsymbol{F}\boldsymbol{P}\boldsymbol{F}^H = \frac{1}{N}\boldsymbol{W}\boldsymbol{F}\boldsymbol{P}\boldsymbol{F}^H$, or $\boldsymbol{Y}_f^H = \frac{1}{N}\boldsymbol{F}\boldsymbol{P}\boldsymbol{F}^H\boldsymbol{W}^H$ under $\mathcal{H}_0$. Therefore, the columns of $\boldsymbol{Y}_f^H$ are independent Gaussian random vectors with zero mean and covariance matrix $\frac{\sigma^2}{N^2}\boldsymbol{F}\boldsymbol{P}\boldsymbol{F}^H$, and the product $\boldsymbol{Y}_f^H\boldsymbol{Y}_f$ follows a complex central Wishart distribution with M degrees of freedom:

$$\frac{N^2}{\sigma^2}\boldsymbol{Y}_f^H\boldsymbol{Y}_f \sim \mathcal{CW}(\boldsymbol{F}\boldsymbol{P}\boldsymbol{F}^H, M). \tag{51}$$

The density of the largest eigenvalue of this matrix is given by [41, expression (41)], where we must note that the scale

[11] The probability of detection (P_{D}) is defined as the probability of deciding $\mathcal{H}_1$ when the hypothesis $\mathcal{H}_1$ is true.

matrix $\boldsymbol{F}\boldsymbol{P}\boldsymbol{F}^H$ in (51) has two eigenvalues: 1 with multiplicity B, and 0 with multiplicity $N-B$. If $f_{\text{BLFF}}(\lambda)$ denotes such density, the probability of false alarm is given by

$$P_{\text{FA}} = 1 - \int_0^{\gamma} f_{\text{BLFF}}(\lambda) d\lambda \tag{52}$$

which enables us to set the threshold γ for a prescribed P_{FA}.

The computation of the probability of detection involves finding the distribution of the largest eigenvalue of the matrix $\boldsymbol{Y}_f^H \boldsymbol{Y}_f$, which is non-central Wishart distributed under $\mathcal{H}_1$. To the best of our knowledge, no simple means is known to compute the marginal density of the largest eigenvalue of non-central correlated complex Wishart matrix where the eigenvalues of the scale matrix have multiplicity greater than one (see [42, Sec. 2.1] and references therein, also [41]). It is therefore more convenient to assess the performance empirically, as described in Sec. VII-C.

C. CM and CMBL detectors

From (32), (41) and (44) we see that the detectors exploiting the CM property rely on the (2,1)-subordinate matrix norm of a correlated Gaussian matrix. To the best of the authors' knowledge, the distribution of this norm remains an open problem in statistics/random matrix theory, so that the threshold of these detectors cannot be determined analytically. However, due to the invariance to scalings of all the detectors presented in the paper, the distributions of the corresponding statistics under $\mathcal{H}_0$ are independent of the noise power so that the threshold required to obtain some target P_{FA} can be computed off-line by means of Monte Carlo simulations. This procedure is the one followed in [9], [19]; see also [11] for more details.

VIII. Simulation Results

Among the detection schemes that have been proposed in the literature (see Sec. I), the statistical performance of only a few of them has been exactly characterized in terms of analytical expressions. More precisely, most of them have been analyzed either approximately, asymptotically, or even heuristically. Notable exceptions include the energy detector [11] and, in this paper, the BL detector. This means that comparisons between different schemes should not be carried out in terms of analytical expressions; instead we must rely on Monte Carlo simulations. In particular, we analyze the performance of the proposed and existing tests in the context of WM signal detection, following the guidelines of the IEEE 802.22 Working Group [29].

A. Simulation Setting

The guidelines in [29] consider six simulation scenarios, termed *test vectors*, which are summarized in Table I. The frequency-modulated analog WM signal $x^*(t)$ is generated according to

$$x^*(t) = \exp\left\{ j \left(2\pi f_c t + \frac{\Delta f}{f_m} \sin(2\pi f_m t), \right) \right\},$$

where Δf is the frequency deviation and f_m is the modulating frequency. This signal is then sampled at rate f_s resulting in $x[n] = x(n/f_s)$. A sampling frequency of $f_s = 6$ MHz is used unless otherwise stated. Zero-mean spatially and temporally white noise with variance σ^2 is added to the signal samples.

#	Description	f_m	Δf	Fading
1	Outdoor, LOS, Silent	32	5	No
2	Outdoor, LOS, Soft Speaker	3.9	15	No
3	Outdoor, LOS, Loud Speaker	13.4	32.6	No
4	Indoor, NLOS, Silent	32	5	Yes
5	Indoor, NLOS, Soft Speaker	3.9	15	Yes
6	Indoor, NLOS, Loud Speaker	13.4	32.6	Yes

TABLE I: Test vectors employed in WM simulation [29]. Frequency units are kHz in all cases.

Frequency-flat channels are considered in all cases. The channel is line-of-sight (LOS) for test vectors 1-3, assuming a uniform linear array (ULA) architecture with half-wavelength spacing: $\boldsymbol{h} = \alpha \cdot [1 \;\; e^{j\theta} \;\; e^{j2\theta} \;\; \cdots \;\; e^{j(M-1)\theta}]^T$, where $\theta \sim \mathcal{U}(0,\pi)$ is a random phase and α^2 determines the power of the signal term. For the test vectors 4-6 vectors, the channel is non-line-of-sight (NLOS) with Rayleigh fading: $\boldsymbol{h} \sim \mathcal{CN}(\boldsymbol{0}, \alpha^2 \boldsymbol{I})$. The SNR (per antenna) is defined as

$$\text{SNR} = \frac{\text{E}\left\{|h_m|^2\right\}}{\text{E}\left\{|w_m[n]|^2\right\}} = \frac{\alpha^2}{\sigma^2}. \tag{53}$$

The values of SNR considered are around -20 dB, corresponding to a very demanding scenario for WM detection (see, e.g., [12], [14]). As simulations reveal, in order to satisfy typical nominal performance requirements in a 6 MHz channel using the proposed BL, BLFF or CMBL detectors necessitates a sensing time in the order of a fraction of millisecond, depending on several factors such as the number of antennas.

In Sec. VIII-B, we compare the proposed detectors with a representative part of the detectors existing in the literature. Results show the advantages of exploiting simultaneously the WM signal features along with the spatial structure provided by the use of multiple antennas. Then in Sec. VIII-C we focus on the novel detectors, illustrating their performance in a wide variety of scenarios.

B. Comparison with Existing Detectors

We now compare the multiantenna WM detectors proposed in this paper with some of the most relevant multiantenna detectors in the literature. The setting considered uses Test Vector 5 with $M = 4$ antennas, $N = 1024$ samples per antenna (corresponding to an observation time of 0.17 ms) and central frequency uniformly distributed across Ω_c, which contains the 237 frequencies where a WM may transmit. Fig. 1 shows the ROC of the proposed detectors along with the sphericity detector (Alamgir *et al.* [24]), the λ_1/trace detector in [10], [23], [25] (labeled as Besson), and three detectors by Zeng *et al.*: Zeng 1 [14, Algorithm 1], Zeng 2 [14, Algorithm 2] and Zeng 3 [9]. We note that Zeng 1 and Zeng 2 are detectors referred to in the IEEE 802.22 standard as blind detectors, whereas Zeng 3 is specifically proposed for

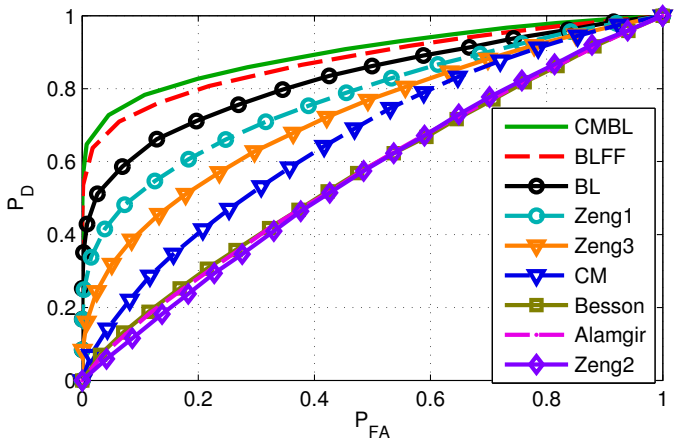

Fig. 1: Test Vector 5, $N = 1024$, B= 200 kHz, $f_s = 6$ MHz, Rayleigh Channel, SNR = -20 dB, $M = 4$.

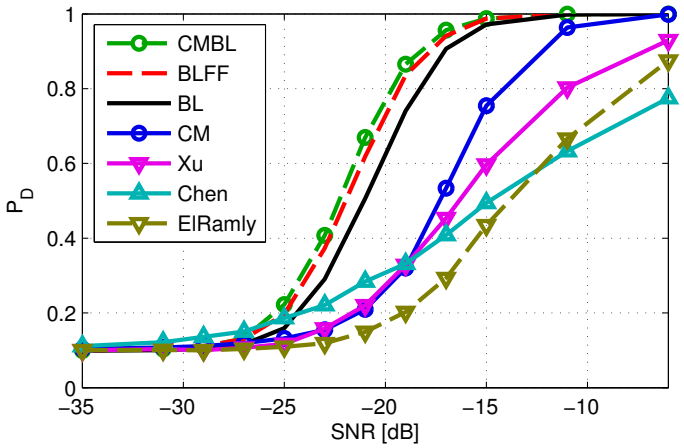

Fig. 2: Test Vector 5, $N = 1024$, B= 200 kHz, $f_s = 6$ MHz, Rayleigh Channel, $M = 4$.

detection of WM signals[12] [4].

We recall that, for a given P_{FA}, detector A is said to perform better than detector B in a given setting if P_{D} is higher for detector A than for detector B. In Fig. 1 it is seen that the three proposed multiantenna WM detectors that exploit the bandwidth information (BL, BLFF and CMBL) outperform all of the previous detectors in the literature. On the other hand, the CM detector is outperformed by Zeng 1 and Zeng 3, which rely on space-time correlation. This shows that temporal correlation is more important than the CM property for WM signal detection.

In order to compare the proposed detectors with existing single-antenna WM detectors, Fig. 2 depicts P_{D} *vs.* SNR when $P_{\text{FA}} = 0.1$ for the BL, BLFF, CM and CMBL detectors along with the detector by Xu *et al.* [17], the detector by ElRamly *et al.* [21] and the one by Chen *et al.* [19]. The threshold of each detector is set to achieve $P_{\text{FA}} = 0.1$. The advantages of using several antennas are clear: not only is the P_{D} of the multiantenna detectors better, but also the *rate* at which P_{D} increases as the SNR improves[13]. Among the four detectors proposed, the performance of the CM detector shows a significant gap with respect to the other three. This effect will be further discussed in Sec. VIII-C.

C. Performance of the Proposed Detectors

In order to illustrate independently the impact of each parameter on the performance of the detectors, in the simulation experiments here we vary one parameter at a time keeping the remaining ones fixed. In particular, for the sake of comparison with other detectors we start assuming that $\Omega_c = \{2\pi f_c/f_s\}$, i.e., the only one candidate frequency is the carrier frequency. Later, we consider the influence of the cardinality of this set and the technique explained at the beginning of Sec. VI-B.

[12]Note that, although the detectors by Zeng *et al.* were proposed in the IEEE 802.22 standard for single-antenna detection, we are considering the multiantenna extensions given by the authors. This, together with the fact that these detectors stem from *ad-hoc* considerations, explains why in the multiantenna scenario of Fig. 1, Zeng 3 performs worse than Zeng 1.

[13]This is related to the well-known concept of *diversity* in multiantenna communications [43].

In order to illustrate the benefits of multiantenna detectors, Fig. 3 shows the influence of the number of antennas M on the probability of detection for fixed $P_{\text{FA}} = 0.1$ and SNR $= -24$ dB. With the exception of the CM detector, the proposed schemes exhibit a significant improvement as M increases, thus showing that in this setting the BL property is more useful for detection purposes than the CM property. This effect stems from the fact that the fractional bandwidth of the WM signal is small for the sampling rate considered (200 kHz/6 MHz $= 1/30$). With larger fractional bandwidths, the advantage of the BL property over the CM property diminishes. This is illustrated in Fig. 4, where the probability of detection is depicted *vs.* the sampling frequency in the range 200 kHz $\leq f_s \leq$ 2 MHz for $P_{\text{FA}} = 0.1$. With fixed WM signal bandwidth ($b = 200$ kHz), the net effect is the variation of the fractional bandwidth b/f_s. In the extreme case where $f_s = 200$ kHz the sampled signal ceases to be bandlimited, and it is observed that the detectors exploiting the CM property show a better P_{D} than those which do not. In fact, the BL detector is unable to detect the signal at all since the only property it exploits is absent in the signal. The performance of the BLFF at this point is slightly better since it exploits the spatial correlation. As the sampling rate is increased, the fractional bandwidth of the signal decreases, and thus the BL property becomes more relevant. Note that the performance of the CM detector is not affected by the fractional bandwidth, as could be expected. In addition, the performance of the BLFF detector approaches that of CMBL for sufficiently small fractional bandwidths; in particular, for $f_s = 30 \cdot 200$ kHz $= 6$ MHz, the performance of both schemes is similar, although the computational cost of BLFF is considerably lower.

Next we complete the performance evaluation in terms of the simulation scenarios in Table I. Fig. 5 shows the ROC curves corresponding to the six test vectors for the BLFF detector when SNR$= -22$ dB and the number of antennas is $M = 4$. It is observed that the probability of detection does not meaningfully depend on the parameters of the WM signal (modulating frequency and frequency deviation). It is the channel model which essentially determines the performance

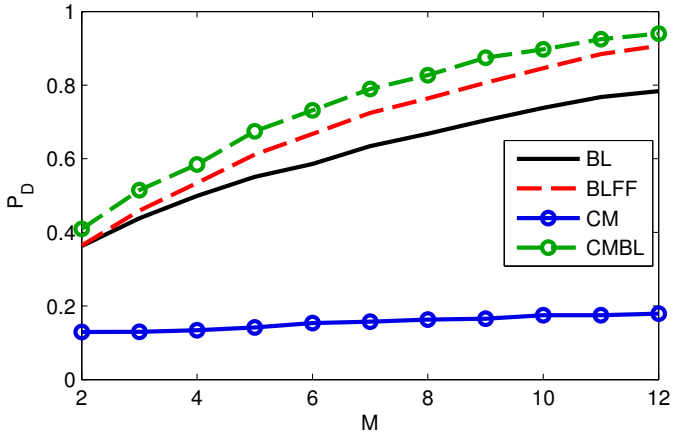

Fig. 3: $N = 1024$, B= 200 kHz, $f_s = 6$ MHz, Test Vector 5, Rayleigh Channel, SNR = -24 dB.

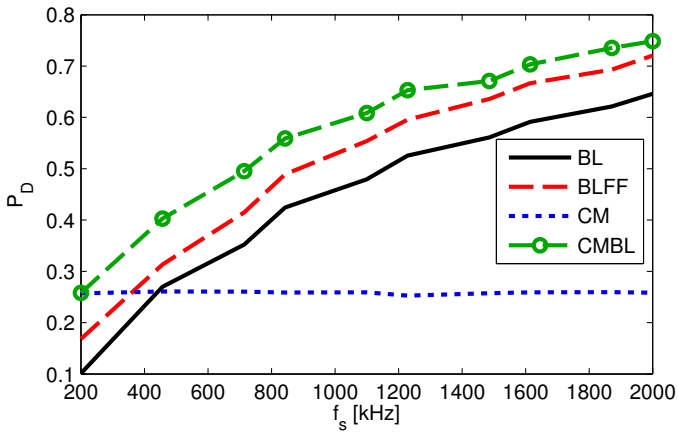

Fig. 4: $N = 1024$, B= 200 kHz, $f_s = 200$ kHz, Test Vector 5, Rayleigh Channel, SNR = -20 dB, $M = 4$.

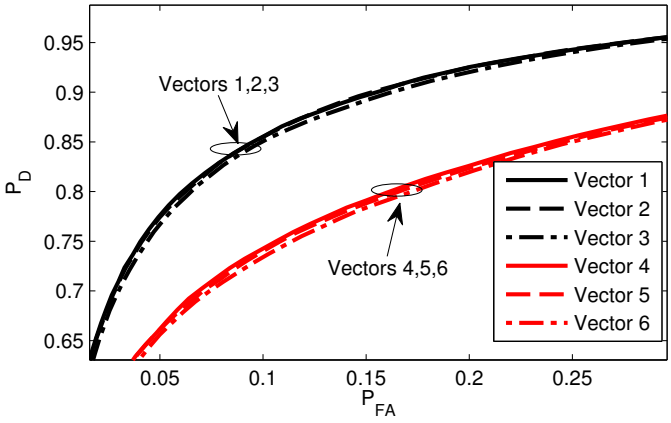

Fig. 5: $N = 1024$, B= 200 kHz, $f_s = 6$ MHz, SNR = -22 dB, $M = 4$, BLFF.

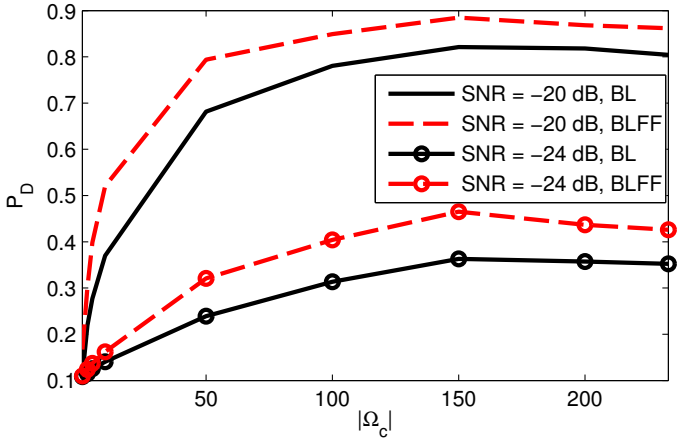

Fig. 6: $N = 1024$, B= 200 kHz, $f_s = 6$ MHz, Test Vector 5, Rayleigh Channel, $M = 4$.

of the detector to a larger extent. This agrees with intuition, since detecting a signal in the presence of a LOS component should be easier than when operating under NLOS conditions. Although not shown for brevity, a similar behavior is observed for the BL, CM, and CMBL detectors.

To close this section we analyze the tradeoff discussed in Sec. VI-B by considering multiple candidate carrier frequency values, *i.e.,* $|\Omega_c| > 1$. As pointed out, it is not strictly necessary to scan the 237 central frequencies using the theoretical bandwidth of 200 kHz. Instead, we can reduce the number of candidate frequency intervals by increasing their width. In the experiment reported in Fig. 6, this approach is followed by dividing the 6 MHz channel into $|\Omega_c|$ intervals. Specifically, for $|\Omega_c| = n$ intervals, we consider the following candidate carrier frequency set and bandwidth:

$$\Omega_c^{(n)} = \left\{ \frac{2\pi}{n} k, \quad k = 0, 1, \ldots, n-1 \right\}, \quad \mathcal{B}^{(n)} = \frac{2\pi}{n}. \quad (54)$$

When the WM signal is present, its carrier frequency is taken as $f_c = 0$. It is observed in Fig. 6, where P_{FA} was set to 0.1, that the probability of detection stabilizes when $|\Omega_c|$ is large enough. This observation allows computational savings at a small performance loss, since the complexity of some of the proposed schemes increases linearly with the number of candidate frequency intervals. Of course, other choices for $\Omega_c^{(n)}$ and $\mathcal{B}^{(n)}$ different from (54) may be preferable in practice depending on the desired tradeoff. It is also observed that the probability of detection slightly decreases after $|\Omega_c|$ is about 150. This is a consequence of the fact that when the number of candidate frequencies is too high, the probability that the actual frequency is erroneously estimated becomes larger.

IX. Conclusions

The protection of wireless microphone users is a requirement for emerging dynamic spectrum access systems operating in TV white spaces. Whereas no previous WM detector considers the use of multiple antennas, none of the multiantenna detectors in the literature have been specifically designed for WM signals. In order to fill this gap we have developed four GLR-based multiantenna detectors which exploit a number of WM signal features. The computational load of these detectors increases with the amount of WM signal structure that they exploit, and therefore they offer different tradeoffs between performance and complexity.

The proposed detectors do not require synchronizing with the potentially present WM signal, and are robust to the noise uncertainty problem as well as to small-scale fading due to the use of multiple antennas. No knowledge of any parameter (channel coefficients, transmitted signal, noise power) is required. Performance was analyzed theoretically and using Monte Carlo simulations. The proposed schemes are well behaved and outperform previous detectors, in particular those proposed in the IEEE 802.22 standard for WM detection.

APPENDIX
COMPUTATION OF $||\boldsymbol{Y}^H||_{2,1}^2$

Consider the constrained maximization problem (29). The cost can be written explicitly as

$$\begin{aligned} J(\boldsymbol{g}) = ||\boldsymbol{Y}^H\boldsymbol{g}||_1 &= \sum_{n=0}^{N-1} |\boldsymbol{y}^H[n]\boldsymbol{g}| \\ &= \sum_{n=0}^{N-1} \sqrt{\boldsymbol{g}^H\boldsymbol{y}[n]\boldsymbol{y}^H[n]\boldsymbol{g}}. \end{aligned} \quad (55)$$

One must maximize (55) subject to $\boldsymbol{g}^H\boldsymbol{g} = 1$. The corresponding Lagrangian is

$$\mathcal{L}(\boldsymbol{g}, \lambda) \doteq J(\boldsymbol{g}) - \frac{\lambda}{2}(\boldsymbol{g}^H\boldsymbol{g} - 1), \quad (56)$$

where λ is the Lagrange multiplier. Note that the gradient of the constraint is $2\boldsymbol{g}$, which does not vanish on the unit sphere $||\boldsymbol{g}||_2 = 1$. It follows that all feasible points are regular, and any local extremum of the constrained problem must satisfy the first-order necessary conditions $\nabla_{\boldsymbol{g}}\mathcal{L}(\boldsymbol{g}, \lambda) = 0$, $\nabla_{\lambda}\mathcal{L}(\boldsymbol{g}, \lambda) = 0$, which are readily seen to yield $\nabla_{\boldsymbol{g}}J(\boldsymbol{g}) = \lambda\boldsymbol{g}$, $\boldsymbol{g}^H\boldsymbol{g} = 1$. The gradient of J is given by

$$\nabla_{\boldsymbol{g}}J(\boldsymbol{g}) = \sum_{n=0}^{N-1} \frac{\boldsymbol{y}[n]\boldsymbol{y}^H[n]}{|\boldsymbol{y}^H[n]\boldsymbol{g}|}\boldsymbol{g} = \boldsymbol{A}(\boldsymbol{g}) \cdot \boldsymbol{g}, \quad (57)$$

where we have introduced the $M \times M$ matrix

$$\boldsymbol{A}(\boldsymbol{g}) \doteq \sum_{n=0}^{N-1} \frac{\boldsymbol{y}[n]\boldsymbol{y}^H[n]}{|\boldsymbol{y}^H[n]\boldsymbol{g}|} = \boldsymbol{Y}\boldsymbol{D}^{-1}(\boldsymbol{g})\boldsymbol{Y}^H, \quad (58)$$

with $\boldsymbol{D}(\boldsymbol{g}) \doteq \operatorname{diag}\left\{ |\boldsymbol{y}^H[0]\boldsymbol{g}| \;\; |\boldsymbol{y}^H[1]\boldsymbol{g}| \cdots |\boldsymbol{y}^H[N-1]\boldsymbol{g}| \right\}$. Note that $\boldsymbol{A}(\boldsymbol{g})$ is positive (semi)definite, and that the cost (55) can be written as $J(\boldsymbol{g}) = \boldsymbol{g}^H\boldsymbol{A}(\boldsymbol{g})\boldsymbol{g}$.

The first-order necessary conditions read then as

$$\boldsymbol{A}(\boldsymbol{g})\boldsymbol{g} = \lambda\boldsymbol{g}, \qquad \boldsymbol{g}^H\boldsymbol{g} = 1. \quad (59)$$

Thus we see that at any extremum of the constrained problem, $\boldsymbol{g}$ must be a unit-norm eigenvector of $\boldsymbol{A}(\boldsymbol{g})$. The corresponding eigenvalue is the attained cost, i.e. $J(\boldsymbol{g}) = \boldsymbol{g}^H\boldsymbol{A}(\boldsymbol{g})\boldsymbol{g} = \lambda$. These conditions do not reveal whether λ corresponds to the largest, smallest, or an intermediate eigenvalue of $\boldsymbol{A}(\boldsymbol{g})$. However, by examining the high SNR case, for which $\boldsymbol{Y} \approx \boldsymbol{h}\boldsymbol{x}^H(\phi)$, one sees that $\boldsymbol{A}(\boldsymbol{g}) = \boldsymbol{Y}\boldsymbol{D}^{-1}(\boldsymbol{g})\boldsymbol{Y}^H \approx [\boldsymbol{x}^H(\phi)\boldsymbol{D}^{-1}(\boldsymbol{g})\boldsymbol{x}(\phi)]\boldsymbol{h}\boldsymbol{h}^H$, i.e. a rank-1 matrix, whose eigenvector associated to the largest eigenvalue is the true channel vector $\boldsymbol{h}$ (independently of $\boldsymbol{g}$). Therefore, it makes sense to consider numerical methods for the computation of the principal eigenvector of a matrix, and then update the matrix at each iteration by using the eigenvector estimate from the previous step. For example, the standard power method [37] can be suitably modified in this manner, see Table II.

TABLE II: Modified Power Method

Set $\boldsymbol{g}_0 =$ principal eigenvector of $\boldsymbol{Y}\boldsymbol{Y}^H$
for $k = 1$ to n_iter **do**
$\quad \boldsymbol{v}_k = \boldsymbol{A}(\boldsymbol{g}_{k-1})\boldsymbol{g}_{k-1}$
$\quad \boldsymbol{g}_k = \frac{\boldsymbol{v}_k}{||\boldsymbol{v}_k||}$
end for
Set $\hat{\boldsymbol{g}} = \boldsymbol{g}_{n\_\text{iter}}$

A reasonable initializer for any numerical method of this kind is the eigenvector associated to the largest eigenvalue of $\boldsymbol{Y}\boldsymbol{Y}^H$, since this is the solution to (29) if we relax the ℓ^1-norm to the ℓ^2-norm in the cost function. In addition, since all elements of $\boldsymbol{x}(\phi)$ have unit magnitude, in the high SNR regime one has $\boldsymbol{D}(\boldsymbol{g}) \approx |\boldsymbol{h}^H\boldsymbol{g}|\boldsymbol{I}$, so that $\boldsymbol{A}(\boldsymbol{g}) \approx \frac{1}{|\boldsymbol{h}^H\boldsymbol{g}|}\boldsymbol{Y}\boldsymbol{Y}^H$, and thus the eigenvectors of $\boldsymbol{A}(\boldsymbol{g})$ and $\boldsymbol{Y}\boldsymbol{Y}^H$ should lie close to each other.

REFERENCES

[1] Federal Communications Commission, "FCC 08-260," *Unlicensed Operation in the TV Broadcast Bands*, 2008.

[2] Federal Communications Commission, "FCC 10-174," *Unlicensed Operation in the TV Broadcast Bands*, 2010.

[3] Federal Communications Commission, "FCC 11-131," *Unlicensed Operation in the TV Broadcast Bands*, 2011.

[4] "IEEE standard for information technology–local and metropolitan area networks–specific requirements– part 22: Cognitive wireless RAN medium access control (MAC) and physical layer (PHY) specifications: Policies and procedures for operation in the TV bands," pp. 1–680, 2011.

[5] Q. Zhao and B. M. Sadler, "A survey of dynamic spectrum access," *IEEE Signal Process. Mag.*, vol. 24, no. 3, pp. 79–89, 2007.

[6] T. Yucek and H. Arslan, "A survey of spectrum sensing algorithms for cognitive radio applications," *IEEE Commun. Surveys and Tutorials*, vol. 11, no. 1, pp. 116–130, 2009.

[7] E. Axell, G. Leus, E.G. Larsson, and H.V. Poor, "Spectrum sensing for cognitive radio : State-of-the-art and recent advances," *IEEE Signal Process. Mag.*, vol. 29, no. 3, pp. 101–116, May 2012.

[8] Y. C. Liang, K. C. Chen, G. Y. Li, and P. Mahonen, "Cognitive radio networking and commun.: An overview," *IEEE Trans. Veh. Technol.*, vol. 60, no. 7, pp. 3386–3407, 2011.

[9] Y. Zeng and Y. C. Liang, "Spectrum-sensing algorithms for cognitive radio based on statistical covariances," *IEEE Trans. Veh. Technol.*, vol. 58, no. 4, pp. 1804–1815, 2009.

[10] P. Wang, J. Fang, N. Han, and H. Li, "Multiantenna-assisted spectrum sensing for cognitive radio," *IEEE Trans. Veh. Technol.*, vol. 59, no. 4, pp. 1791–1800, May 2010.

[11] S. M. Kay, *Fundamentals of Statistical Signal Process., Vol. II: Detection Theory*, Prentice-Hall, 1998.

[12] D. Cabric, "Addressing feasibility of cognitive radios," *IEEE Signal Process. Mag.*, vol. 25, no. 6, pp. 85–93, 2008.

[13] R. Tandra and A. Sahai, "SNR walls for signal detection," *IEEE J. Sel. Topics Signal Process.*, vol. 2, no. 1, pp. 4–17, 2008.

[14] Y. Zeng and Y. C. Liang, "Eigenvalue-based spectrum sensing algorithms for cognitive radio," *IEEE Trans. Commun.*, vol. 57, no. 6, pp. 1784–1793, 2009.

[15] E. L. Lehmann and J. P. Romano, *Testing statistical hypotheses*, Springer, 2005.

[16] L. L. Scharf, *Statistical signal processing: detection, estimation, and time series analysis*, vol. 1, Addison-Wesley Publishing Company, 1991.

[17] S. Xu, Y. Shang, and H. Wang, "Application of SVD to sense wireless microphone signals in a wideband cognitive radio network," in *2nd Int. Conf. on Signal Process. and Communication Syst.*, 2008, pp. 1–7.

[18] M.H. Hassan and O.A. Nasr, "Adaptive spectrum sensing of wireless microphones with noise uncertainty," in *IEEE 22nd Int. Symposium on Personal Indoor and Mobile Radio Commun.*, 2011, pp. 445–450.

[19] H. Chen and W. Gao, "Spectrum sensing for TV white space in North America," *IEEE J. Sel. Areas Commun.*, vol. 29, no. 2, pp. 316–326, 2011.

[20] H.S. Chen, W. Gao, and D.G. Daut, "Spectrum sensing for wireless microphone signals," in *5th IEEE Annual Commun. Society Conf. on Sensor, Mesh and Ad Hoc Commun. and Networks Workshops*, 2008, pp. 1–5.

[21] S. ElRamly, F. Newagy, H. Yousry, and A. Elezabi, "Novel modified energy detection spectrum sensing technique for FM wireless microphone signals," in *2011 IEEE 3rd Int. Conf. on Communication Software and Networks*, 2011, pp. 59–63.

[22] M. Gautier, M. Laugeois, and D. Noguet, "Teager-Kaiser energy detector for narrowband wireless microphone spectrum sensing," in *Cognitive Radio Oriented Wireless Networks Commun. (CROWNCOM)*, 2010, pp. 1–5.

[23] A. Taherpour, M. Nasiri-Kenari, and S. Gazor, "Multiple antenna spectrum sensing in cognitive radios," *IEEE Trans. Wireless Commun.*, vol. 9, no. 2, pp. 814–823, 2010.

[24] M. Alamgir, M. Faulkner, J. Gao, and P. Conder, "Signal detection for cognitive radio using multiple antennas," in *IEEE Int. Symposium on Wireless Communication Syst.*, 2008, pp. 488–492.

[25] O. Besson, S. Kraut, and L. L. Scharf, "Detection of an unknown rank-one component in white noise," *IEEE Trans. Signal Process.*, vol. 54, no. 7, pp. 2835–2839, Jul. 2006.

[26] D. Ramírez, G. Vázquez-Vilar, R. López-Valcarce, J. Vía, and I. Santamaría, "Detection of rank-P signals in cognitive radio networks with uncalibrated multiple antennas," *IEEE Trans. Signal Process.*, vol. 59, no. 8, pp. 3764–3774, Aug. 2011.

[27] J. Sala-Álvarez, G. Vázquez-Vilar, and R. López-Valcarce, "Multi-antenna GLR detection of rank-one signals with known power spectrum in white noise with unknown spatial correlation," *IEEE Trans. Signal Process.*, vol. 60, no. 6, pp. 3065–3078, 2012.

[28] G. Vázquez-Vilar, R. López-Valcarce, and J. Sala, "Multiantenna spectrum sensing exploiting spectral a priori information," *IEEE Trans. Wireless Commun.*, vol. 10, no. 12, pp. 4345–4355, Dec. 2011.

[29] C. Clanton, M. Kenkel, and Y. Tang, "Wireless microphone signal simulation method," *IEEE 802.22-07/0124r0*, 2007.

[30] T. Erpek, M.A. Mchenry, and A. Stirling, "Dynamic spectrum access operational parameters with wireless microphones," *Commun. Magazine, IEEE*, vol. 49, no. 3, pp. 38–45, 2011.

[31] Federal Communications Commission, "Frequency assignment for low power auxiliary stations," *47 CFR Chapter I, Subchapter C, Part 74, Subpart H, point 74.802*.

[32] M. Derakhtian, A.A. Tadaion, and S. Gazor, "Detection of a bandlimited signal with unknown parameters," in *IEEE/SP 15th Workshop on Statistical Signal Process.*, 2009, pp. 145–148.

[33] M. Derakhtian, A.A. Tadaion, S. Gazor, and MM Nayebi, "Invariant activity detection of a constant magnitude signal with unknown parameters in white Gaussian noise," *IET Commun.*, vol. 3, no. 8, pp. 1420–1431, 2009.

[34] D. Romero and R. López-Valcarce, "Bandlimited or constant envelope? exploiting waveform properties in wireless microphone detection," in *IEEE Int. Workshop Comput. Advances Multi-Sensor Adaptive Process (CAMSAP)*, San Juan, Puerto Rico, Dic. 2011, pp. 321–324.

[35] T. W. Anderson, *An introduction to multivariate statistical analysis*, John Wiley and Sons, 3rd edition, 2003.

[36] J. Demmel, *Applied numerical algebra*, SIAM, Philadelphia, 1997.

[37] G. H. Golub and C. F. Van Loan, *Matrix computations*, vol. 3, Johns Hopkins Univ Pr, 1996.

[38] S. Boyd and L. Vandenberghe, *Convex Optimization*, Cambridge University Press, Cambridge, UK, 2004.

[39] A. N. Kolmogorov and S. V. Fomin, *Introductory Real Analysis Rev. English Ed*, Dover Publications, 1970.

[40] P. P. Vaidyanathan, *Multirate systems and filter banks*, Pearson Education Taiwan, 2003.

[41] A. Zanella, M. Chiani, and M. Z. Win, "On the marginal distribution of the eigenvalues of Wishart matrices," *IEEE Trans. Commun.*, vol. 57, no. 4, pp. 1050–1060, 2009.

[42] R. Couillet and M. Debbah, *Random matrix methods for wireless communications*, Cambridge University Press, 2011.

[43] G. Vázquez-Vilar, R. López-Valcarce, and A. Pandharipande, "Detection diversity of multiantenna spectrum sensors," in *IEEE Int. Conf. Acoust., Speech, Signal Process.*, 2011, pp. 2936–2939.